doi:10.1016/j.jmb.2004.11.015 J. Mol. Biol. (2005) 345, 1131–1139

JMB

Available online at www.sciencedirect.com

SCIENCE DIRECT®

ELSEVIER

The Crystal Structure of Annexin A8 is Similar to that of Annexin A3

Stéphane Réty[1], Jana Sopková-de Oliveira Santos[1,2], Lise Dreyfuss[1,3] Karine Blondeau[4], Katerina Hofbauerová[1,5] Céline Raguénès-Nicol[3,6], Daniel Kerboeuf[3,7], Madalena Renouard[1] Françoise Russo-Marie[3,8] and Anita Lewit-Bentley[1]*

[1]*LURE, Centre Universitaire Paris-Sud, BP 34, 91898 Orsay Cedex, France*

[2]*CERMN, UFR des Sciences Pharmaceutiques, 5 rue Vaubenard, F-14032 Caen France*

[3]*ICGM, U332 INSERM, 22 rue Méchain, 75014 Paris, France*

[4]*IGM, Bât. 360, Centre Universitaire Paris-Sud, 91405 Orsay Cedex, France*

[5]*Institute of Microbiology ASCR, Vídenská 1083, 142 20 Prague 4, Czech Republic*

[6]*Equipe OB, UMR CNRS 6026 Université Rennes I, 35042 Rennes Cedex. France*

[7]*CRI, Bât. 210, Université Paris-Sud, 91405 Orsay Cedex France*

[8]*BIONEXIS, Paris Biotech 4 avenue de l'Observatoire 75006 Paris, France*

**Corresponding author*

Annexin A8 is a relatively infrequent and poorly studied member of this large family of calcium-binding and membrane-binding proteins. It is, however, associated with a specific disease, acute promyelocytic leukemia. We have solved its three-dimensional structure, which includes a moderately long and intact N terminus. The structure is closest to that of annexin A3 and highlights several important regions of inherent flexibility in the annexin molecule. The N terminus resembles that of annexin A3, as it lies along the concave surface of the molecule and inserts partially into the hydrophilic channel in its centre. Since both annexins A3 and A8 are expressed in promyelocytic cells during their differentiation, the similarity in their structures might suggest a functional relationship.

Keywords: annexin; X-ray crystal structure; intact N terminus; cell differentiation

Introduction

Annexins are a family of proteins that bind to membranes in a calcium-dependent manner. Although the physiological role of annexins is still unclear, they are most likely involved in membrane trafficking and fusion. It has been shown that members of the annexin family are expressed in a growth-dependent manner and are targets for cellular kinases, suggesting their involvement in cell proliferation and differentiation.[1]

All members of the annexin family possess a conserved core formed by four homologous repeats of about 70 residues and an N-terminal part that is variable in length and sequence.[2,3] The conserved

Present addresses: M. Renouard, LPS, Centre Universitaire Paris-Sud, Bât 510, 91405 Orsay Cedex, France; S. Réty and A. Lewit-Bentley, LBPA, ENS-Cachan, 61 avenue du Président Wilson, 94235 Cachan, France.

Abbreviations used: GST, glutathione-*S*-transferase; APL, acute promyelocytic leukemia; ATRA, all-*trans* retinoic acid.

E-mail address of the corresponding author: anita.bentley@lure.u-psud.fr

0022-2836/$ - see front matter

core binds calcium and phospholipids, while the N-terminal sequence is considered to be responsible for the specific functions of different annexins. In several annexins it contains phosphorylation sites and in some, such as annexins A1,[4] A2,[5] and A7,[6] the site of interaction with other proteins. Modifications of the N terminus have been shown to influence the membrane-binding properties of the conserved core in some annexins. The atomic structure of the conserved core of many annexins has been determined by high-resolution X-ray crystallography, giving a detailed description of the structure of the four repeat domains and the calcium-binding sites for annexins A1,[7] A2,[8] A3,[9] A4,[10] A5,[11] A6,[12] C7,[13] B12,[14] and D24.[15] The molecule is composed of four structural domains of five α-helices each. The four domains are arranged in a cyclic manner, with domains I and IV, and domains II and III forming two modules separated by a hydrophilic cleft that has been suggested as the site of a voltage-gated calcium channel.[16] The overall shape of the core structure is elongated and slightly curved, with a convex side that contains the calcium-binding sites and a concave side where the N and C termini come together.

As far as the variable N-terminal domain is concerned, however, structural information is much less abundant. The N terminus of annexin A5, the paradigm for all annexins, is one of the shortest, with only ten residues preceding the conserved Phe11, yet the very first two or three residues are disordered in most crystal structures. For annexins containing longer N termini, such as A1, A2 or A7, only the truncated forms yielded crystal structures until very recently.[7] The N terminus of annexin A3 (18 residues) folds along the concave surface of the protein towards the hinge between the core modules and is stabilised by the side-chain of residue Trp5 inserting into the hydrophilic region of the channel, where it forms several salt-bridges and hydrogen bonds.[9] When this residue is mutated to alanine, the N terminus becomes disordered in the crystal structure.[17] Recently, Rosengarth *et al*. have succeeded in obtaining a stable full-length annexin A1, which they have crystallised in the absence and in the presence of calcium.[7,18] They were able to demonstrate a most surprising conformational change involving the N terminus: in the absence of calcium, it inserts into domain III by displacing helix D of that domain. In the presence of calcium, all domains assume their normal topology and, while the N terminus is present in the crystal in its full length, it is totally disordered. Thus, so far, the only information on the conformation of the first 12 residues of the annexin A1 and A2 N termini in the presence of calcium comes from the structures of complexes with their protein partners, the S100 family proteins S100A11 and S100A10, respectively.[19,20] This information is, however, limited to the very N-terminal region only. Annexin A8 has a medium-length N terminus that includes three Trp residues as well as several Ser and Thr residues, one of which is a potential phosphorylation target. The detailed description of its conformation would therefore be of interest for the entire annexin family.

Annexin A8 was first identified as a second gene product together with annexin A5 (then called VAC-α), it was cloned, characterised and named VAC-β.[21] It was detected subsequently in human placenta in very small quantities (less than 1% of all extracted annexins).[22] At the same time, annexin A8 was identified as a gene that is highly and very specifically expressed in cells of patients with acute promyelocytic leukemia (APL),[23] a disease that is characterised by a chromosomal translocation t(15;17)(q21;q22). No annexin A8 expression was detected in other leukemias. Further studies showed that the expression of annexin A8 in NB4 cells, the model cell-line for APL, is regulated by all-*trans* retinoic acid (ATRA), which induces differentiation of these cells.[24] More recently, annexin A8 was identified in two apparently unrelated tissue types: bound to lung lamellar bodies[25] and in chondrocytes in the mammalian growth plate.[26] In all cases, the amount of annexin A8 expressed is very low compared to annexin expression in general, which can attain 1–2% of all protein in some cell types.[1] In several cases where it has been identified, annexin A8 seems to be a marker of cellular differentiation.[24,26]

We have been interested in the study of structure–function relationship of annexins for some time,[27–29] and in particular annexin A3.[9,17,30] The latter is of special interest because of its role in inflammation,[31] as well as in the differentiation of myelomonocytic cell lines,[32] where its expression seems to be complementary to that of annexin A8. We have now extended our structural studies to annexin A8 in two forms, wild-type, whose N terminus is sensitive to proteolysis, and a K16A mutant carrying an intact full-length N terminus.

Results

Annexin A8 expression

In order to produce sufficient quantities of pure annexin A8 for structural and biochemical studies, we tested a semi-automated fermentor procedure of high cell-density culture. Figure 1 summarises the kinetics of bacterial growth and the production of the glutathione-*S*-transferase (GST)-annexin A8 fusion protein produced using two different carbon substrates, glucose or glycerol. A standard protocol in batch culture on LB medium was carried out in parallel. The fed-batch method consistently gave recombinant protein concentrations of one order of magnitude higher than the standard culture, whatever the carbon substrate used, with the protein remaining soluble and giving crystals of equivalent quality.

After analysing the wild-type form, we found the N terminus prone to proteolytic cleavage and

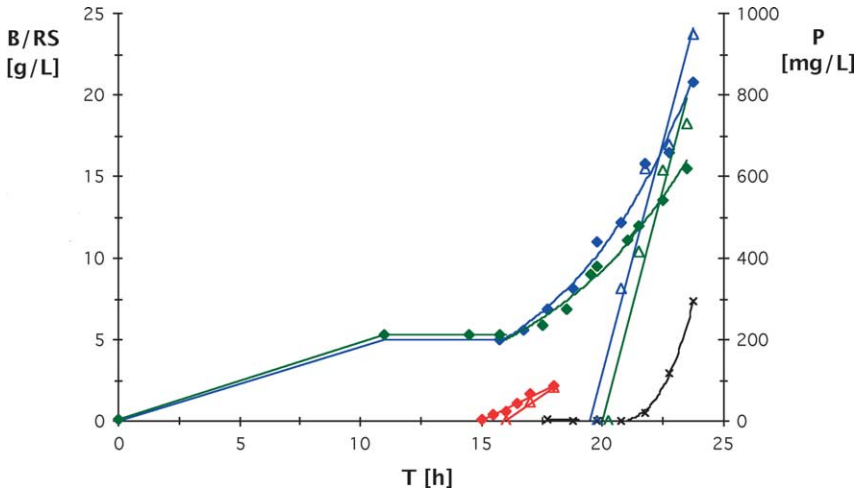

Figure 1. Annexin A8-GST expression in *E. coli* BL21Gold cells. Comparison of two carbon sources, glucose (green) and glycerol (blue). (♦) Growth of bacterial cells; (△) annexin A8-GST expression. In red are the concentrations for a standard batch culture using Luria–Bertani (LB) medium. B, biomass; P, protein (annexin A8-GST). The total recombinant protein concentration of annexin A8-GST produced in the cells was estimated by densitometry (Master total Lab, Amersham Pharmacia Biotech) of 0.1% (w/v) SDS, 12% (w/v) polyacrylamide gels stained with Coomassie brilliant blue, by comparison with a standard quantity of bovine serum albumin.

indeed, the protein recovered from the crystals was incomplete. N-terminal sequencing localised the cleavage to the peptide bond Lys16-Ser17, a cleavage typical of calpain-like proteases (we shall therefore call this form Δ(1–16)).[33] Since we were particularly interested in the structure of the full-length protein, we decided to modify the sequence to Ala-Ser by site-directed mutagenesis (K16A mutant). Subsequent N-terminal sequencing confirmed that the latter protein form was stable over time.

Annexin A8 overall structure

The crystallisation conditions for both forms were similar, with the exception of calcium, present in low concentration in the crystallisation buffer of the Δ(1–16) form. Since the precipitating agent was ammonium sulphate, the amount of free calcium available in solution was limited and thus would not bind to the protein with high occupancy. In spite of the similar crystallisation conditions and the relatively small difference in size of the protein, the crystals do not belong to the same space-group. The Δ(1–16) form crystallised in space-group $P2_1$ (a=50.76 Å, b=65.58 Å, c=59.23 Å, β=100.7°) with one molecule in the asymmetric unit, while the K16A mutant gave crystals in $P1$ (a=49.30 Å, b=59.65 Å, c=70.79 Å, α=84.4°, β=83.3°, γ=74.1°) with two molecules in the asymmetric unit, related by a non-crystallographic 2-fold axis (Tables 1 and 2).

Table 1. Crystallographic data

	Wild-type	K16A mutant
Source	DW32	CuKα
λ (Å)	0.97	1.54
Resolution (Å)	2.10	2.5
No. observations	110,643	94,198
No. unique reflections	22,712	26,449
Data completion	0.985 (0.892)	0.905 (0.914)
R_{merge} [a]	0.065 (0.314)	0.077 (0.287)
$I/\sigma(I)$	21.7 (5.5)	7.58 (2.04)

Values in parentheses refer to the highest-resolution range.
[a] $R_{merge} = \Sigma_h \Sigma_i |I(h)_i - \langle I(h)\rangle| / \Sigma_h \Sigma_i (I(h)_i$.

The overall structure of the core part of annexin A8 is similar to that of other annexins, as expected (Figure 2). When superimposed upon the structures of annexins A1, A3 and A5, using LSQKAB from the CCP4 package, the rms difference in C^α positions is smallest for annexin A3[9] (3.05 Å) and annexin A1 (3.07 Å with the full-length, calcium-bound form,[18] 3.15 Å with the full-length calcium-free form[7]), going up to 6.25 Å with annexin A5.[27] The angle between the modules of domains I+IV and II+III that defines the hydrophilic cleft between them is smaller in annexin A8 than in either A3 or A1, with the latter being the most open structure. The structure of annexin A3 showed a relative twist of domains I and IV with respect to domains II and III,[9] which is not observed in annexin A8.

The loop connecting domains II and III is defined very poorly in both annexin A8 crystal forms. Within the crystal packing this loop lies close to the N terminus of a neighbouring molecule, itself defined rather poorly in parts, in both forms. The connection between domains I and II, on the other hand, is very well defined. It is formed by a short stretch of the sequence Pro-Pro-Tyr-Arg that lies in the hinge region between the annexin modules formed by domains I and IV on one side and domains II and III on the other side. This hinge is rather abrupt, with the Tyr95 side-chain pointing into the space between the modules. Here, its OH group interacts *via* a well-defined water molecule with the side-chain of Asn127. This steric constraint translates, however, into the peptide bond adopting an unfavourable conformation (unfavourable values of angles ϕ, ψ).

Calcium-binding loops

In spite of the presence of calcium in the

Table 2. Refinement statistics

	Wild-type	K16A mutant
R^a	0.175	0.206
R_{free}	0.217	0.269
Non-hydrogen atoms	1514	5053
Calcium ions	1	0
Water molecules	114	27
$\langle B \rangle$ (Å^2)	67.19	34.24
rmsd from ideality		
Bond lengths (Å)	0.011	0.010
Bond angles (deg.)	1.140	1.267
Planes (Å)	0.004	0.004
Chiral volumes (Å^3)	0.066	0.087
Ramachandran plot[b]		
Most-favoured regions (%)	93.7	91.6
Generously allowed regions (%)	5.3	8.4
Additionally allowed regions (%)	0.7	0
Disallowed regions (%)	0.4	0

[a] $R = \Sigma|F_o - F_c|/\Sigma F_o$; R_{free} is as defined;[40] 5% exclusion was used.
[b] Determined by PROCHECK.[41]

crystallising solution of the Δ(1–16) annexin A8 crystal form, we find only one weakly bound calcium ion in the AB loop of domain IV (type II binding site[11]). When refined with 0.5 occupancy, its *B*-factor is 24 Å^2 and its ligand geometry

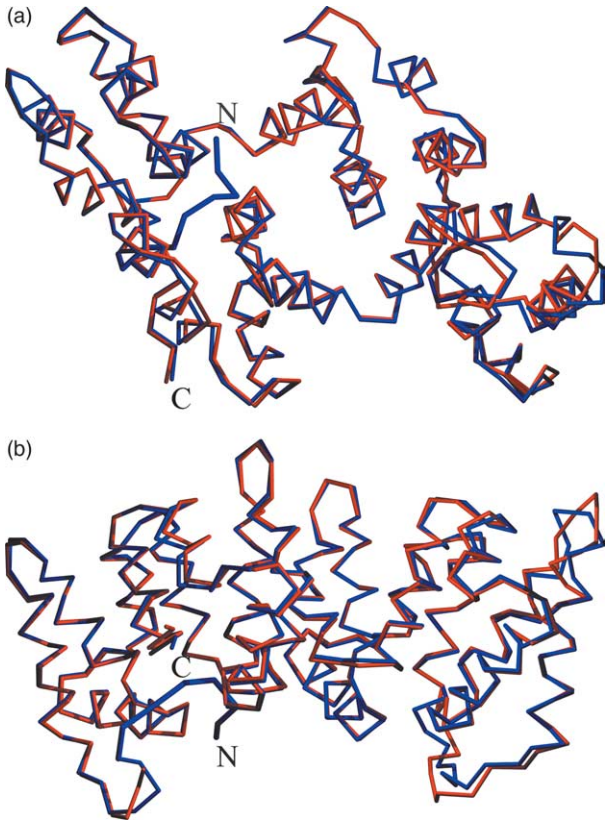

Figure 2. Overall structure of annexin A8. Annexin A8 Δ(1–16) (red) and K16A mutant (blue) were superimposed. The N terminus of K16A mutant extends between domain I and domain IV. The view in B is rotated by 90° from the view in A.

corresponds to typical annexin calcium sites (Figure 3). The AB loops in domains I and II have a water molecule coordinated by the potential calcium ligands in the calcium site. The coordination is complete for the AB loop in domain II, but in domain I the carbonyl oxygen atom of Lys35 points away from the water molecule. In the crystal packing, an AB loop of domain I lies "upside-down" against an AB loop of domain II of a symmetry-related molecule (Figure 4). The planes of the two loops are approximately perpendicular, the water molecules in the calcium positions lie 4.3 Å from each other, with a third water molecule hydrogen bonded to both of them. Leu109 at the top of the domain II loop inserts 4.1 Å from Thr74 and 5.4 Å from Met34 side-chains of the opposite molecule. Similarly, Ile37 at the top of the domain I loop lies at 3.5 Å from Ala149 of the opposite molecule, all these interactions contributing to the stabilisation of the conformation of these two loops.

On the other hand, the AB loop in domain III has very poorly defined electron density, the carbonyl oxygen atoms of the loop and the carboxyl group of Glu235 do not point towards the calcium site at all. However, even if no calcium ion is visible inside this loop, Arg194, the equivalent of Trp190 and Trp187 in annexins A3 and A5, respectively, is exposed to solvent, which is consistent with a conformation ready to bind calcium. In the K16A mutant crystals, which were grown in the absence of calcium, no ion is found in the AB loops, as expected. The loop of domain III is in a closed, or buried conformation, with Arg194 pointing to the interior of the molecule and making a hydrogen bond with the carbonyl oxygen atom of Lys233 (Figure 5).

Structure of the N terminus

The full-length N terminus of the K16A mutant behaves in a fairly similar way in the two molecules of the unit cell, but there are a few differences. These translate into an rms difference between the C$^\alpha$ atoms of the two molecules of 2.176 Å in this region, while it is only 0.513 Å for the entire structure. The electron density is better defined in molecule A from Ser17 to Thr14, then becomes very tenuous up to Ile8. On the other hand, the electron density is more continuous from residue Gly12 to Ile8 in molecule B. In both molecules, the chain comes back into contact with the surface of the molecule at the base of domain I, then extends towards domain IV at the closed part of the hydrophilic channel up to Gln10 (Figure 2). This region of the N terminus is better defined, stabilised by backbone hydrogen bonds between the carbonyl oxygen atom of Gln10 and peptide nitrogen atoms of Ser284 and Glu285. At this point the chain turns back to the surface of the molecule and the rest of the N terminus is disordered, since no electron density is visible.

The side-chain of Gln10 extends into the hydrophilic channel, forming hydrogen bonds with the carboxyl group of Glu98 and the hydroxyl group of

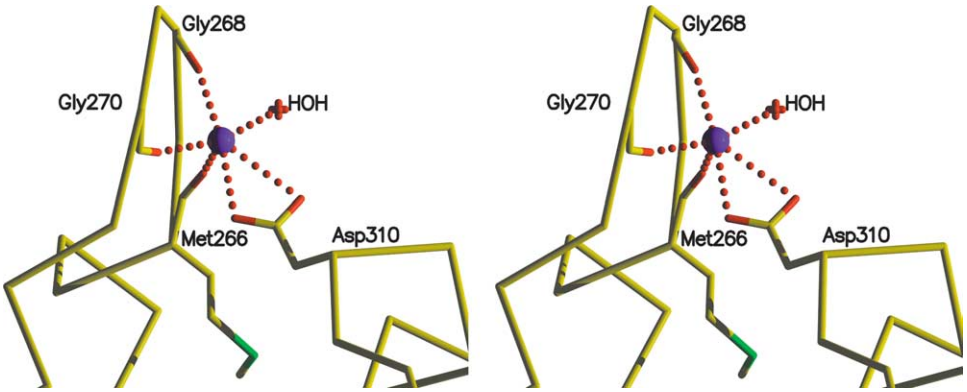

Figure 3. The AB loop in domain IV of annexin A8 wt. The calcium ion (purple) is coordinated by carbonyl oxygen atoms of Met266, Gly268 and Gly70, and the carboxyl group of Asp310. A water molecule plays the role of the sixth ligand.

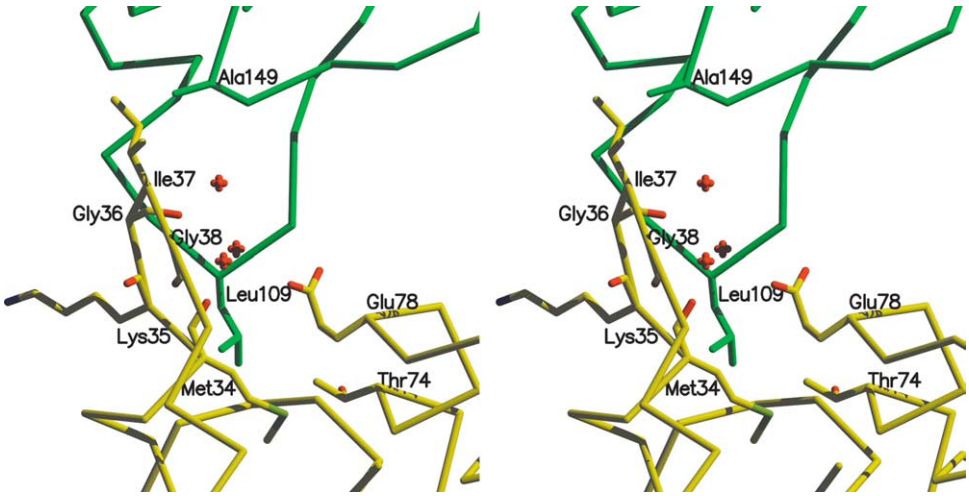

Figure 4. Crystal packing of AB loops in domain I of one molecule (yellow) and domain II of a symmetry-related molecule (green).

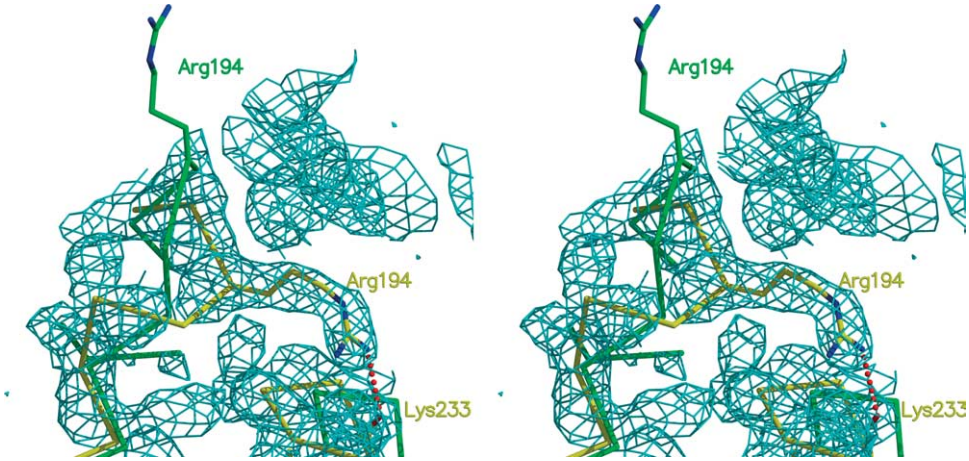

Figure 5. The AB loop of domain III in Δ(1–16) (green) and K16A mutant (yellow). The electron density of K16A mutant ($2F_o - F_c$, 1σ) is shown.

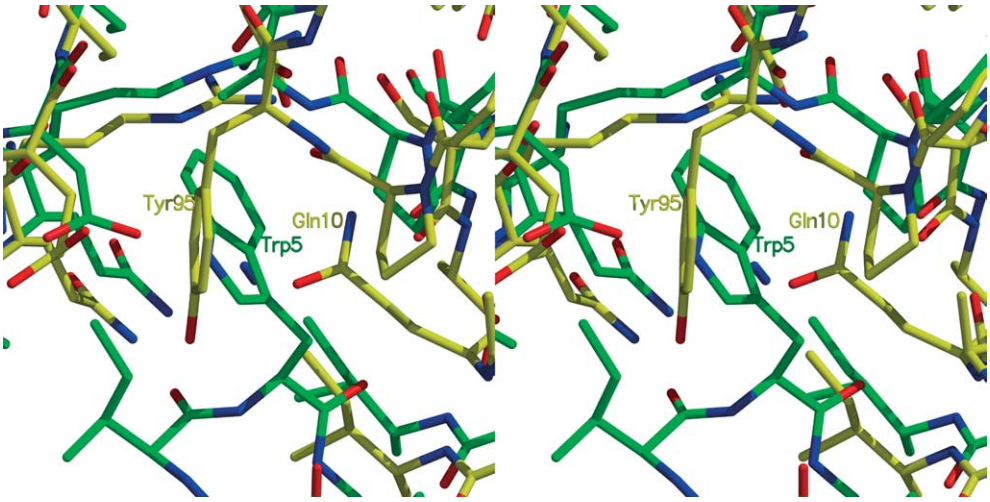

Figure 6. Superposition of annexin A3 (green) and annexin A8 (yellow) in the region of Trp5/Gln10.

Ser282 from domain IV. When the structure of the wild-type annexin A3 is superimposed, the Gln10 side-chain of annexin A8 lies within 2 Å of Trp5 of annexin A3 (Figure 6). The Tyr95 side-chain of annexin A8 overlaps with a part of the indole ring of Trp5 of annexin A3.

Discussion

We have solved the structures of two forms of annexin A8, a Δ(1–16) form crystallised in the presence of a small amount of calcium, and a K16A mutant form without any calcium present. It has been notoriously difficult to obtain annexin crystals in the total absence of calcium and thus it is of interest to analyse structural differences in the case of annexin A8. The C^{α} atoms of the two crystal forms superpose with an overall rms difference of 0.865 Å. The largest difference, of 5.7 Å, is localised at Arg194 which lies at the extremity of the AB loop in domain III (Figure 5). This is a smaller amplitude than that observed for annexin A5, where the equivalent Trp187 moves by 9 Å from the closed to the open conformation.[34] The case of annexin A5 may be considered as one extreme, where the closed conformation is stable even in the presence of low concentrations of calcium. The transition to the open conformation, which involves a concomitant movement of 12 Å of the DE loop, requires a high concentration of calcium, low pH or the presence of a membrane surface.[35] At the other extreme lies the remarkable rearrangement of the entire domain III in annexin A1 caused by the presence or absence of calcium.[7,18] The fact that even a very small concentration of calcium is sufficient to induce a change in the conformation of domain III in annexin A8 as well suggests that domain III plays a key role in the inherent flexibility and thereby in the function of annexins.

The structure of annexin A8 is closest to annexin A3 structure and, indeed, these two annexins share key structural features in the N-terminal region. Like Trp5 of annexin A3, Gln10 could serve to lock the two modules of annexin A8 *via* internal hydrogen bonds and thus block the hinge-opening movement between the modules.[17] Interestingly, the calcium-containing form lacks the first 16 residues of its N terminus and, in particular, Gln10. The conformational change in the AB loop of domain III described above may thus be facilitated by, if not actually caused by, increased flexibility of the molecule due to the absence of the N-terminal sequence.

The precise function of the N terminus of annexin A8 is not known. The N-terminal part of annexin A8 may be a target for phosphorylation, proteolysis, binding to a cellular partner or a combination of these regulation systems. The region susceptible to proteolysis in annexin A8 is indeed very accessible on the surface of the protein and clearly very flexible, as its electron density is defined poorly in both structures we have analysed. Proteolytic cleavage in annexins, in particular by calpain, has been considered recently as physiologically relevant.[36] The authors suggest that, since both annexins and calpain locate to cell membranes in the presence of calcium, controlled proteolysis of the N termini of some annexins could serve to modulate the N terminus-dependent specific functions of these annexins. A PEST motif (a sequence rich in Pro, Glu, Ser and Thr) was predicted between residues 20 and 32 in the N-terminal part of the protein. The score value according to Barnes *et al*.[36] and PESTFind[37] is rather low, and it has yet to be proved that poor PEST sequences are really signals for proteolysis. We did however observe differences during the purification of Δ(1–16) annexin A8 and the K16A mutant. Both proteins were expressed as GST fusion proteins. The yield for Δ(1–16) annexin A8 was low and the fermentor strategy had been adopted to obtain sufficient amounts of protein for structural studies. Proteolytic cleavage could have occurred during the extraction step, separating the GST moiety from the annexin before the affinity purification step. On

the other hand, the yield for K16A mutant was high and no problem of expression was encountered, which correlates with the stability of its N terminus.

No S100 protein has been shown to be associated with annexin A8 even if an increase in the molecular mass of 10 kDa was observed during the purification of the protein from placenta.[22] The N terminus composition of annexin A8 is different from those of A1 and A2, however, and cannot form an amphipathic helix capable of interacting with S100 proteins. Thr14 may be a PKC phosphorylation site as predicted by Hauptmann *et al*.[21] and confirmed by NetPhos.[38] The function of phosphorylation is not known, but it could modify the hinge movement of the core part of the structure, and thus its membrane-associated activity. The presence of a potential proteolytic cleavage site removing the N-terminal 16 residues strengthens the hypothesis that this region is particularly important for the regulation of the activity of annexin A8.

Annexins A8 and A3 were known to have common biochemical properties, since they copurify from placenta[22] and we now show that their structures are very similar as well. The level of annexin A3 increases during differentiation of promyelocytic cell lines,[39] and it has been shown that annexin A8 is overexpressed in APL[23] and is repressed at the transcription level during ATRA induction[24] at early stages of differentiation. Annexin A8 thus may have specific functions in undifferentiated cells. On the other hand, White *et al*.[26] have shown that annexin A8 is a marker of chondrocyte differentiation but have not verified the level of annexin A3 in these cells. It is possible that these two annexins are not expressed at the same time and are mutually exclusive. Given our structural results, we suggest that annexins A8 and A3, with their subtle structural differences, may have related functions in some cells undergoing differentiation.

Conclusions

The three-dimensional structure of annexin A8 is remarkably similar to that of annexin A3, in particular in its potential of regulating the inter-module flexibility of the molecule. The structure of the K16A mutant of annexin A8 reveals the conformation of an intact medium-length annexin N terminus, including two highly accessible functional regulation sites, a calpain cleavage site and a potential phosphorylation site. In both cases, the regulation would take place by releasing the N terminus from restrictive interactions within the hydrophilic channel between the annexin structural modules, releasing their full flexibility. Since both annexins A3 and A8 are expressed in promyelocytic cells during their differentiation, the similarity in their structures might suggest a functional relationship.

Material and Methods

Annexin A8 expression

Annexin A8 cDNA was obtained from a cDNA insert purified using the Qiaquick PCR purification kit from QIAGEN and cloned into the pGEX-2T vector. The K16A mutation was obtained by PCR using the synthetic oligonucleotide 5′-PGGT GTC ACA GTG GCG AGC AGC TCC CCA CTT C-3′. The mutation was checked by DNA sequencing.

The Δ(1–16) annexin A8 expression was carried out in an Applikon fermentor system in fed-batch cultures of the *Escherichia coli* strain BL21λDE3-Gold (Stratagene). Cell cultures of 1500 ml were carried out in a modified synthetic M63 medium, at pH 7, a temperature of 37 °C, stirring rate of 1200 revs/minute and an aeration of 1 vvm (volume of air per volume of culture per minute). Two carbon sources were tested, glucose and glycerol, in order to optimise protein production. The feeding profile of medium was calculated to maintain a specific growth rate of $0.25\,h^{-1}$. Recombinant protein production was induced with 1 mM IPTG for two hours when the absorbance at 600 nm reached 20 a.u. (i.e. about 10 g/l of biomass). In parallel, standard (batch culture) expression was carried out as well: a 1 l culture of *E. coli* BL21λDE3 (Stratagene) transformed with the appropriate plasmid was induced with 0.2 mM IPTG when the absorbance reached 0.9 a.u. at 600 nm. Bacteria were lysed in 30 ml of TENGN (50 mM Tris (pH 7.4), 1 mM EDTA, 100 mM NaCl, 1% (v/v) NP40, 10% (v/v) glycerol, 1 mM DTT, 0.5 mg/ml of lysozyme) supplemented with protease inhibitors (2 μg/ml of aprotinin, 1 mM PMSF, 2 μg/ml of leupeptin, 2 μg/ml of pepstatin, 40 μg/ml of trypsin inhibitor). Lysis was carried out with a French press for the fed-batch culture and by mild sonication for the batch culture. The soluble fraction was purified by incubation with gluthatione beads (SIGMA) overnight, then washed. The annexin A8 moiety was cleaved in 50 mM Tris–HCl (pH 8), 200 mM NaCl by 900 units of thrombin for one hour at 37 °C with stirring. The sample was desalted into 50 mM Tris–HCl (pH 8), 1 mM EDTA, 1 mM EGTA and loaded onto a Resource Q (Pharmacia) column, then eluted with a NaCl gradient up to 0.25 M. The final purification step involved size-exclusion chromatography on a Superdex 75 column (Pharmacia). Purity was checked by SDS-PAGE and the protein concentrated on Centricon concentrators (Amicon) to 20 mg/ml in 50 mM Tris–HCl (pH 8.0), 1 mM EDTA, 150 mM NaCl.

Crystallisation and structure determination

Crystals were obtained using the hanging-drop, vapour-diffusion technique at 18 °C, mixing 1 μl of protein solution with 1 μl of reservoir solution. In the case of Δ(1–16) annexin A8, the reservoir solution contained 50 mM cacodylate buffer (pH 6), 10 mM $CaCl_2$, 45% (w/v) ammonium sulphate. The K16A mutant crystallised from 0.1 M Tris (pH 7.5), 2 M ammonium sulphate, 2% PEG 400.

Data collections were carried out on the DW32 station of LURE, DCI, for the Δ(1–16) crystals and on a Rigaku MicroMax 007 rotating anode source for the K16A mutant crystals. Both instruments were equipped with a MAR345 imaging plate. The Δ(1–16) and K16A crystals were measured at room temperature. All data were treated with the HKL programme package,[39] followed by programmes from the CCP4 suite.[40]

The structures were solved by molecular replacement (AMoRe from the CCP4 suite), followed by refinement. The search model for the Δ(1–16) structure was prepared by homology modelling using the ExPASy (Expert Protein Analysis System) proteomics server of the Swiss Institute of Bioinformatics[41] with the structure of annexin A3[9] as a template. The refined Δ(1–16) coordinates were then used as a search model for the K16A mutant structure. The molecular replacement solution for the Δ(1–16) structure was first refined with XPLOR,[42] followed by REFMAC from the CCP4 suite. The latter programme was used for the K16A mutant structure refinement.

Protein Data Bank accession codes

The coordinate and structure factors files have been deposited with the PDB under ID codes 1w3w (Δ(1–16)) and 1w45 (K16A mutant).

Acknowledgements

The financial contribution of the European Commission contract BIO4-CT-96-0083 is acknowledged. K.H. acknowledges financial support from the French Ministère d'Affaires Etrangères. We are grateful to the group of Jean-Luc Popot at the IPBC, Paris, especially Ines Gallay and Daniel Picot, for allowing us to collect data on their X-ray equipment. The staff of LURE are acknowledged for running the synchrotron facility.

References

1. Raynal, P. & Pollard, H. B. (1994). Annexins: the problem of assessing the biological role for a gene family of multifunctional calcium- and phospholipid-binding proteins. *Biochim. Biophys. Acta*, **1197**, 63–93.
2. Moss, S. E. (1992). *The Annexins*, Portland Press, London.
3. Gerke, V. & Moss, S. E. (2002). Annexins: from structure to function. *Physiol. Rev.* **82**, 331–371.
4. Mailliard, W. S., Haigler, H. T. & Schlaepfer, D. D. (1996). Calcium-dependent binding of S100C to the N-terminal domain of annexin I. *J. Biol. Chem.* **271**, 719–725.
5. Johnsson, N., Marriott, G. & Weber, K. (1988). p36, the major cytoplasmic substrate of src tyrosine protein kinase, binds to its p11 regulatory subunit via a short amino-terminal amphiphatic helix. *EMBO J.* **7**, 2435–3442.
6. Brownawell, A. M. & Creutz, C. E. (1997). Calcium-dependent binding of sorcin to the N-terminal domain of synexin (annexin VII). *J. Biol. Chem.* **272**, 22182–22190.
7. Rosengarth, A., Gerke, V. & Luecke, H. (2001). X-ray structure of full-length annexin 1 and implications for membrane aggregation. *J. Mol. Biol.* **306**, 489–498.
8. Burger, A., Berendes, R., Liemann, S., Benz, J., Hofmann, A., Gottig, P. *et al*. (1996). The crystal structure and ion channel activity of human annexin II, a peripheral membrane protein. *J. Mol. Biol.* **257**, 839–847.
9. Favier-Perron, B., Lewit-Bentley, A. & Russo-Marie, F. (1996). The high-resolution crystal structure of human annexin III shows subtle differences with annexin V. *Biochemistry*, **35**, 1740–1744.
10. Zanotti, G., Malpeli, G., Gliubich, F., Folli, C., Stoppini, M., Olivi, L. *et al*. (1998). Structure of the trigonal crystal form of bovine annexin IV. *Biochem. J.* **329**, 101–106.
11. Huber, R., Römisch, J. & Pâques, E. (1990). The crystal and molecular structure of human annexin V, an anticoagulant protein that binds to calcium and membranes. *EMBO J.* **9**, 3867–3874.
12. Kawasaki, H., Avila-Sakar, A., Creutz, C. E. & Kretsinger, R. H. (1996). The crystal structure of annexin VI indicates relative rotation of the two lobes upon membrane binding. *Biochim. Biophys. Acta*, **1313**, 277–282.
13. Liemann, S., Bringemeier, I., Benz, J., Gottig, P., Hofmann, A., Huber, R. *et al*. (1997). Crystal structure of the C-terminal tetrad repeat from synexin (annexin VII) of *Dictyostelium discoideum*. *J. Mol. Biol.* **270**, 79–88.
14. Luecke, H., Chang, B. T., Maillard, W. S., Schlaepfer, D. D. & Haigler, H. T. (1995). Crystal structure of the annexin XII hexamer and implications for bilayer insertion. *Nature*, **378**, 512–515.
15. Hofmann, A., Proust, J., Dorowski, A., Schantz, R. & Huber, R. (2000). Annexin 24 from Capsicum annuum. X-ray structure and biochemical characterization. *J. Biol. Chem.* **275**, 8072–8082.
16. Berendes, R., Vosges, D., Demange, P., Huber, R. & Burger, A. (1993). Structure-function analysis of the ion channel selectivity filter in human annexin V. *Science*, **262**, 427–430.
17. Hofmann, A., Raguénès-Nicol, C., Favier-Perron, B., Mesonero, J., Huber, R., Russo-Marie, F. & Lewit-Bentley, A. (2000). The annexin A3-membrane interaction is modulated by an N-terminal tryptophan. *Biochemistry*, **39**, 7712–7721.
18. Rosengarth, A. & Luecke, H. (2003). A calcium-driven conformational switch of the N-terminal and core domains of annexin A1. *J. Mol. Biol.* **326**, 1317–1325.
19. Réty, S., Sopkova, J., Renouard, M., Osterloh, D., Gerke, V., Tabaries, S. *et al*. (1999). The crystal structure of a complex of p11 with the annexin II N-terminal peptide. *Nature Struct. Biol.* **6**, 89–95.
20. Réty, S., Osterloh, D., Arie, J. P., Tabaries, S., Seeman, J., Russo-Marie, F. *et al*. (2000). Structural basis of the Ca(2+)-dependent association between S100C (S100A11) and its target, the N-terminal part of annexin I. *Struct. Fold. Des.* **8**, 175–184.
21. Hauptmann, R., Maurer-Fogy, I., Krystek, E., Bodo, G., Andree, H. & Reutelingsperger, C. P. M. (1989). Vascular anticoagulant beta: a novel human Ca^{2+}/phospholipid binding protein that inhibits coagulation and phospholipase A2 activity. Its molecular cloning, expression and comparison with VAC-alpha. *Eur. J. Biochem.* **185**, 63–71.
22. Pepinsky, F. B. & Hauptmann, R. (1992). Detection of VAC-β (annexin-8) in human placenta. *FEBS Letters*, **306**, 85–89.
23. Chang, K. S., Wang, G., Freireich, E. J., Daly, M., Naylor, S. L., Trujillo, J. M. & Stass, S. A. (1992). Specific expression of the annexin VIII gene in acute promyelocytic leukemia. *Blood*, **79**, 1802–1810.
24. Sarkar, A., Yang, P., Fan, Y. H., Mu, Z. M., Hauptmann, R., Adolf, G. R. *et al*. (1994). Regulation of the expression of annexin VIII in acute promyelocytic leukemia. *Blood*, **84**, 279–286.
25. Sohma, H., Ohkawa, H., Akino, T. & Kuroki, Y. (2001).

Binding of annexins to lung lamellar bodies and the PMA-stimulated secretion of annexin V from alveolar type II cells. *J. Biochem.* **130**, 449–455.
26. White, A. H., Watson, R. E. B., Newman, B., Freemont, A. J. & Wallis, G. A. (2002). Annexin VIII is differentially expressed by chondrocytes in the mammalian growth plate during endochondral ossification and in osteoarthritic cartilage. *J. Bone Miner. Res.* **17**, 1851–1858.
27. Sopkova, J., Renouard, M. & Lewit-Bentley, A. (1993). The crystal structure of a new high-calcium form of annexin V. *J. Mol. Biol.* **234**, 816–825.
28. Liemann, S. & Lewit-Bentley, A. (1995). Annexins: a novel family of calcium- and mambrane-binding proteins in search of a function. *Structure*, **3**, 233–237.
29. Oling, F., Sopkova-de Oliveira Santos, J., Govorukhina, N., Mazères-Dubut, C., Bergsma-Schutter, W., Oostergetel, G. *et al*. (2000). Structure of membrane bound annexin A5 trimers: a hybrid Cryo-EM–X-ray crystallography. *J. Mol. Biol.* **304**, 561–573.
30. Sopkova, J., Raguénès-Nicol, C., Vincent, M., Chevalier, A., Lewit-Bentley, A., Russo-Marie, F. & Gallay, J. (2002). Ca^{2+} and membrane binding to annexin 3 modulate the structure and dynamics of its N-terminus and domain III. *Protein Sci.* **11**, 1613–1625.
31. Coméra, C., Rothhut, B., Cavadore, J. C., Vilgrain, I., Cochet, C., Chambaz, E. & F., R.-M. (1989). Further characterization of four lipocortins from human peripheral blood mononuclear cells. *J. Cell Biochem.* **40**, 361–370.
32. Coméra, C., Rothhut, B. & R.-M., F. (1990). Identification and characterization of phospholipase A2 inhibitory proteins in human mononuclear cells. *Eur. J. Biochem.* **188**, 139–146.
33. Tompa, P., Buzder-Lantos, P., Tantos, A., Farkas, A., Szilagyi, A., Banoczi, Z. *et al*. (2004). On the sequential determinants of calpain cleavage. *J. Biol. Chem.* **279**, 20775–20785.
34. Sopkova-De Oliveira Santos, J., Fischer, S., Guilbert, S., Lewit-Bentley, A. & Smith, J. (2000). Pathway for large-scale conformational change in annexin V. *Biochemistry*, **39**, 14065–14074.
35. Sopkova, J., Vincent, M., Takahashi, M., Lewit-Bentley, A. & Gallay, J. (1999). Conformational flexibility of domain III of annexin V at membrane/water interface. *Biochemistry*, **38**, 5447–5458.
36. Barnes, J. A. & Gomes, A. V. (2002). Proteolytic signals in the primary structure of annexins. *Mol. Cell. Biochem.* **231**, 1–7.
37. Rechsteiner, M. & Rogers, S. W. (1996). PEST sequences and regulation by proteolysis. *Trends Biochem. Sci.* **21**, 267–271.
38. Blom, N., Gammeltoft, S. & Brunak, S. (1999). Sequence- and structure-based prediction of eukaryotic protein phosphorylation sites. *J. Mol. Biol.* **294**, 1351–1362.
39. Otwinowski, Z. & Minor, W. (1997). Processing of X-ray diffraction data collected in oscillation mode. In *Macromolecular Crystallography* (Carter, C. W. & Sweet, R. M., eds), vol. 276, pp. 307–326, Academic Press, New York.
40. Collaborative Computational Project, Number4. (1994). The CCP4 suite: programs for protein crystallography. *Acta Crystallog. sect. D*, **50**, 760–763.
41. Bates, P. A., Kelley, L. A., MacCallum, R. M. & Sternberg, M. J. E. (2001). Enhancement of protein modelling by human intervention in applying the automatic programs 3D-JIGSAW and 3D-PSSM. *Proteins: Struct. Funct. Genet.* **5**, 39–46.
42. Brünger, A. T. (1988). *X-PLOR Manual*, Howard Hughes Medical Institute and Department of Molecular Biophysics and Biochemistry, Yale University, New Haven, CT.

Edited by R. Huber

(Received 31 August 2004; received in revised form 3 November 2004; accepted 8 November 2004)